Proceedings of the 2005 IEEE
International Conference on Robotics and Automation
Barcelona, Spain, April 2005

# Natural Gait Generation Techniques for Multi-bodied Isolated Mechanical Systems

Elie Shammas
*Mechanical Engineering Department*
*Carnegie Mellon University*
*Pittsburgh, PA 15213, U.S.A.*
*eshammas@andrew.cmu.edu*

Klaus Schmidt
*Institute of Automation and Control*
*University of Erlangen-Nuremberg*
*Erlangen, Germany*
*klaus.schmidt@rt.eei.uni-erlangen.de*

Howie Choset
*Mechanical Engineering Department*
*Carnegie Mellon University*
*Pittsburgh, PA 15213, U.S.A.*
*choset@cs.cmu.edu*

***Abstract*— This paper investigates how to generate cyclic gaits for multi-bodied isolated mechanical systems whose configuration space is represented by a trivial fiber bundle. We describe how to generate gaits in the base space of the fiber bundle, or the shape space of the robot on which we assume full control. Such gaits are guaranteed to generate a non-zero motion along the fiber space, i.e., a net change in the position of the robot, while making sure that the robot's shape is unchanged after a complete cycle. The gait generation technique presented in this paper is intuitive; it involves dividing the base space into well defined regions and devising a set of simple rules on how to generate curves in such regions. Not only do such curves guarantee non-zero position change but also do allow for gait optimization.**

## I. Introduction

The mechanics of locomotion of multi-bodied robots has been widely studied in the literature, [1], [6], [8]. Most of the related work focuses on connections and how base space motions (shape changes) relate to fiber space motions (position changes). While many types of robots have been studied, the main focus in the prior work has been on robotic systems with non-holonomic constraints [7] and dissipative external forces [4]. Moreover, Lagrangian invariance was exploited to project the dynamics of the entire robotic system onto the smaller dimensional base space. Then the group motions were recovered from the base space motions via a reconstruction equation which is governed by specific "connections". The main goal of most prior work has been to solve for the position change for a given shape change. However, very few tried to solve the "reverse" problem [7], [8], i.e., solving for the base space motion given a desired position change.

In this paper, we attempt to tackle this reverse problem for purely mechanical systems. We design curves or gaits in the base space of the configuration fiber bundle that will yield the desired fiber motion. This is done by first dividing the base space into well defined regions. Then we devise a set of intuitive rules to design curves in the base space. Finally we prove that the designed curves are guaranteed to generate the desired fiber motion. The set of rules governing the gait generation process are simple enough that we have flexibility in generating gaits. This feature will come in handy when we add configuration constraints to our robotic systems.

This paper is organized as follows. In Section II, we present some prior work and background material necessary for understanding the paper. In Section III we introduce the general concept of our approach for generating gaits. Then we present an example with a three-link snake robot in Sections IV and V. Then we simulate these gaits to compute the phase shift and we determine several optimized gaits in Section VI. Finally, we give some future work directions and conclude in Section VII.

## II. Prior Work and Background Material

Our work builds upon prior work done by Ostrowski [7] and Walsh [8]. Walsh has studied the dynamics of a three link robot floating in space (Fig. 1(a)). By writing the Lagrangian of this *specific* system in a special form, Walsh was able to generate gaits for a planar three link snake robot. Walsh has proposed sinusoidal gaits and then computed the phase shift produced by these gaits. In Figure 1(b), we see several circular gaits moving along the $\sigma_1 = \sigma_2$ line where $\sigma_i$ are the relative angles between the links. Note that the computed phase shift increases in magnitude as the gaits move away from the origin.

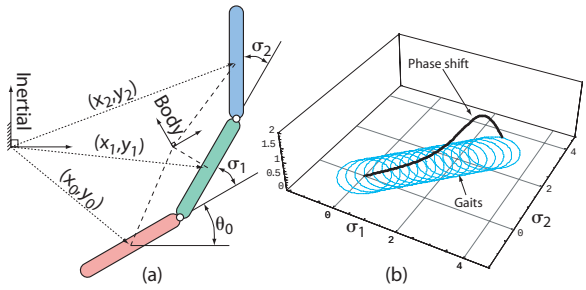


Fig. 1. (a) Coordinates describing the configuration of the three link snake robot. (b) Gaits proposed by Walsh[8].

In this paper, we analyze the same mechanical system proposed by Walsh and generate a richer set of gaits. Instead of writing a specific Lagrangain form for each new mechanical system we use reduction methods presented by Ostrowski to generalize this step. Moreover, we relate the magnitude of the phase shift to a volume integral under a

well defined height function. Hence, not only our method justifies the plot of phase shift magnitude seen in Fig. 1(b), but also allows us to optimize gaits. Now we shall introduce several mechanics of locomotion concepts[1], [7].

### A. Principal bundles

The configuration space of all mechanical systems has a trivial fiber bundle structure. According to [1], a configuration is the minimum number of variables needed to uniquely specify the location in two or three dimensions of each physical point of the mechanism or robot. For robots that are made up of many rigid bodies, variables specifying the robot's shape as well as the robot's position are needed. Often, the position variables are elements of a set that has a group structure as well as a configuration manifold structure. Hence the position variables are governed by a Lie group structure such as $SE(2)$. A general configuration manifold for mechanical systems is usually denoted by $Q = (G, M)$, where $G$ is the Lie group specifying the position of the robot and $M$ is the base space specifying the shape of the robot. In this paper we will deal with configuration manifolds that have a *fiber bundle* structure.

*Definition 1 (Fiber bundle):* A manifold $Q$ with a base subspace $M$ and a projection map $\pi : Q \to M$ is a fiber bundle if for every $r \in M$ there exists a neighborhood $U \subset M$ and $r \in U$ such that:

$$\pi^{-1}(U) \text{ is homeomorphic to } Y \times U,$$

where $Y = \pi^{-1}(r)$, i.e., locally, $Q \cong Y \times M$. Fiber $Y$ is defined as the pre-image of $r \in M$ under the map $\pi$.

Note that if the fiber $Y$ has a group structure then $Q$ is a *principal* fiber bundle, and if $Q = Y \times M$ globally, then $Q$ is a *trivial* fiber bundle. The configuration space of all mechanical systems has trivial principal bundle structure.

### B. Purely mechanical systems

Purely mechanical systems are systems whose motion is governed solely by momentum conservation. Moreover mechanical systems are systems whose Lagrangian is the difference between kinetic energy and potential energy. For the rest of this paper we will assume that the potential energy is zero. Hence, the Lagrangian for purely mechanical system can be written in a quadratic form

$$L(q, \dot{q}) = \frac{1}{2}\dot{q}^T M(q)\dot{q}, \tag{1}$$

where $M(q)$ is the mass matrix of the mechanical system.

### C. Lagrangian invariance and reduction

The concept of invariance of the Lagrangian is crucial for exploiting conservation laws for mechanical systems. The invariance of the Lagrangian with respect to a Lie group action is called *symmetry*, this invariance is equivalent to a conservation law (according to Noether's Theorem [7]). Momentum conservation is due to invariance with respect to translational group actions. Symmetry can be exploited to "simplify" the equations of motion describing the dynamics of the system. The formal definition of invariance is

*Definition 2 (Lagrangian function):* A Lagrangian function $L : TQ \to \mathbb{R}$ is said to be $G-$ invariant if

$$L(\Phi_g(q), T_q\Phi_g(\dot{q})) = L(q, \dot{q}), \tag{2}$$

where $\Phi_g(q)$ and $T_q\Phi_g(\dot{q})$ are respectively the action and lifted action of the Lie group $G$ on the manifold $Q$.

The invariance of the Lagrangian can be used to compute the *reduced Lagrangian* which does not depend on group variables and where group velocities are represented in the body frame of the robot. According to [7], the reduced Lagrangian is given by

$$\begin{aligned} l(\xi^b, r, \dot{r}) &= L((g^{-1}g, r), (T_g\Phi_{g^{-1}}\dot{g}, \dot{r})), \\ &= \frac{1}{2}\begin{pmatrix} \xi & \dot{r} \end{pmatrix}^T \tilde{M}(r) \begin{pmatrix} \xi & \dot{r} \end{pmatrix}, \end{aligned} \tag{3}$$

where $\xi$ is the body velocity representation of $\dot{g}$, i.e., $\xi = T_gL_{g^{-1}}\dot{g}$. Moreover, $\xi$ is a Lie algebra element since $\xi \in T_eG \cong \mathfrak{g}$. Hence, the reduced mass matrix which corresponds to the reduced Lagrangian can be written in the following form

$$\tilde{M}(r) = \begin{pmatrix} I(r) & I(r)A(r) \\ A^T(r)I^T(r) & m(r) \end{pmatrix} \tag{4}$$

where $A(r)$ is the local form of the mechanical connection, $I(r)$ is the local form of the locked inertia tensor[1], and $m(r)$ is a matrix depending only on base variables. Hence, the equations of motion associated with the reduced Lagrangian are [4] [7]:

$$\frac{d}{dt}\left(\frac{\partial l}{\partial \dot{r}^i}\right) - \frac{\partial l}{\partial r^i} = \tau_i \tag{5}$$

where $\tau_i$'s are the input torques of the base variables. This equation constitutes the dynamic equations for the base space.

### D. Connections

For mechanical systems we can define a mechanical connection

$$\mathcal{A}(q, \dot{q}) = \mathbb{I}^{-1}(q)J(\dot{q}), \tag{6}$$

where $\mathbb{I}(q)$ is the locked inertia tensor and $J(\dot{q})$ is the momentum map. The reader is referred to [1] for further details. For trivial fiber bundles, the connection can be written in a local trivialization.

*Proposition 1:* Let $\mathcal{A}$ be a connection form over a trivial fiber bundle[2]. Then $\mathcal{A}$ can be written as

$$\mathcal{A}(q, \dot{q}) = \mathbb{I}^{-1}(q)J(\dot{q}) = Ad_g(T_gL_{g^{-1}}\dot{g} + A(r)\dot{r}), \tag{7}$$

$\forall q = (g, r) \in Q$ where $A(r)$ is called the local form of the connection seen in (4).

[1] $I(r) = \mathbb{I}(e, r)$ where $\mathbb{I}$ is the locked inertia tensor.

[2] The proposition can be seen in [1], however it is proven for principal connections, nonetheless it still applies for mechanical connections on trivial principal fiber bundles.

## III. General Concept

We are interested in generating gaits for rigid multi-bodied robots. We require such gaits to be cyclic. By cyclic we mean that the base variables return to the same configuration after one cycle. Note that we distinguish between the angular configurations 0 and $2\pi$. We use cyclic gaits because we want to design gaits that generate nonzero phase shift after a complete cycle in the base space. In other words, the robot will retain its original shape after one cycle, but its position along the fiber will have changed. Hence, by effectively controlling the base variables, on which we assume full control, we are able to also control the unactuated fiber variables. A second practical reason is that most robots have wires connecting adjacent links and cyclic gaits will not damage these wires.

In the case where there are no constraints and no external forces in the group directions, the equations of motion on the base space are given in (5). Moreover, starting with zero initial momentum, $J(\dot{q}_0)$ and having the robot isolated from all external forces, we know that $J(\dot{q}) = 0$ for all $t$. The motion along the group is determined by the reconstruction equation, (7), which now has the from:

$$\xi = T_g L_{g^{-1}} \dot{g} = -A(r)\dot{r}. \tag{8}$$

This means that there is a direct relation between the base velocities $\dot{r}$ and the group velocities $\dot{g}$.

In this paper we want to concentrate on the type of systems described by Equations 5 and 8 with the Lie group $SE(2)$. Cyclic control input trajectories shall be used for producing net motion along the fibers. We also require that the local form of the connection can be represented as a set of one forms which are zero in the $x$ and $y$ direction (position) and which are nonzero in the $\theta$ direction (orientation)[3], i.e.,

$$A(r) = \begin{pmatrix} 0 & \cdots & 0 \\ 0 & \cdots & 0 \\ f_1(\sigma_1, \ldots, \sigma_m) & \ldots & f_m(\sigma_1, \ldots, \sigma_m) \end{pmatrix}. \tag{9}$$

Rewriting the last row of (8), we get

$$\xi_3 = -\left(f_1 d\sigma_1 + f_2 d\sigma_2 + \ldots + f_m d\sigma_m\right) = \omega \tag{10}$$

From Equation 8 and with $G = SE(2)$ we know that $\xi_3 = \dot{\theta}$. To compute the phase shift, $\Delta\theta$, in the $\theta$ direction for a time interval from $t_1$ to $t_2$, we integrate (10).

$$\Delta\theta = \theta(t_2) - \theta(t_1) = \int_{t1}^{t2} \dot{\theta} dt = -\int_{\partial N} \sum_{i=1}^{m} f_i d\sigma_i = -\int_{\partial N} \omega, \tag{11}$$

where $\partial N$ denotes the input trajectory. Using Stoke's Theorem, the line integral in (11) can be transformed into an area integral over the area of the manifold $N$ bounded by the input trajectory $\partial N$ [5].

$$\int_{\partial N} \omega = \int_{N} d\omega, \tag{12}$$

[3]This a restrictive assumption, our future work will address a more relaxed version.

where $d\omega$ is the exterior derivative of the one-form $\omega$.

$$d\omega = \sum_{i,j=1,i<j}^{m} \left(\frac{\partial f_j}{\partial \sigma_i} - \frac{\partial f_i}{\partial \sigma_j}\right)(d\sigma_i \wedge d\sigma_j). \tag{13}$$

The integral can then be written as

$$\Delta\theta = \sum_{i,j=1,i<j}^{m} \int\int_{A_{ij}} F_{ij} d\sigma_i d\sigma_j, \tag{14}$$

where $F_{ij} = \frac{\partial f_j}{\partial \sigma_i} - \frac{\partial f_i}{\partial \sigma_j}$ and the $A_{ij}$ are projections of the input trajectory on the $\sigma_i - \sigma_j$-plane.

In our approach, we will exploit the properties of the *height functions* $F_{ij}$ to synthesize the input trajectories. Also, we will optimize the gaits to obtain a maximal phase shift with minimum input effort for some cost function.

## IV. Three Link Snake Robot

In this section we will work out a detailed example and compute most of the terms presented above that will be used for evaluating the phase shift.

### A. Configuration

Referring to Fig. 1(a), we have a three-link snake robot. This robot has 5 degrees of freedom, two translational and three rotational. We attach the origin of a body coordinate frame to the center of mass of the entire robot and align its x-axis with the first link of the robot. Hence, the three variables described above, $x$, $y$, and $\theta$, represent a generalized position of the snake robot. Moreover, $g = (x, y, \theta) \in SE(2)$ is a Lie group. We need two more variables to describe the shape of the snake robot, $r = (\sigma_1, \sigma_2) \in \mathbb{S}^1 \times \mathbb{S}^1$, which represent the relative angles between the links. Finally, the configuration of the robot is represented by the *generalized* coordinates $q = (g, r) = (x, y, \theta, \sigma_1, \sigma_2)$, [2]. Also note that the configuration space has a trivial fiber bundle structure where $Q = G \times M = SE(2) \times \mathbb{S}^1 \times \mathbb{S}^1$.

### B. Kinetic energy metric and mass matrix

The right metric to compute the dynamics of the system is nothing but the kinetic energy metric. The kinetic energy of the system is given by

$$KE = \frac{1}{2} \sum_{i=0}^{2} \left(m_i(\dot{x}_i^2 + \dot{y}_i^2) + j_i \dot{\theta}_i^2\right),$$

where $m_i$ is the mass of each link, $j_i$ is the inertia of each link around its center of mass, $(\dot{x}_i, \dot{y}_i)$ is the inertial translational velocity of the center of mass of each link, and $\dot{\theta}_i$ is the inertial angular velocity of each link. However, we would like to write the kinetic energy in terms of the generalized coordinates defined above. This is done by a simple coordinate transformation:

$$x = \sum_{i=1}^{3} x_i \quad ; \quad y = \sum_{i=1}^{3} y_i;$$
$$\theta = \theta_0 \; ; \; \sigma_1 = \theta_1 - \theta \quad ; \quad \sigma_2 = \theta_2 - \theta - \sigma_1;$$

### C. Local form of the connection

Having computed the mass matrix, we can verify that the kinetic energy or Lagrangian, $L(q,\dot{q}) = \frac{1}{2}\dot{q}^T M \dot{q}$, is G-invariant by evaluating both sides of (2). Moreover, we can compute the reduced Lagrangian by (3). For this particular example, the reduced and original Lagrangians are identical[4]. Hence, we can conclude that the reduced mass matrix defined in (1) is the same as the original mass matrix defined in (4), $\tilde{M} = M$. Having computed the reduced mass matrix, the local form of the connection can be directly computed using (4), $A = (I^{-1})(IA) = \tilde{M}_{11}^{-1}\tilde{M}_{12}$. The local form of the connection for the three link snake robot is

$$A = \begin{pmatrix} 0 & 0 \\ 0 & 0 \\ f_1(\sigma_1,\sigma_2) & f_2(\sigma_1,\sigma_2) \end{pmatrix}, \text{ where} \qquad (15)$$

$$\begin{aligned} f_1 &= \frac{6j + 8ml^2 + ml^2(3\cos\sigma_1 + 6\cos\sigma_2 + \cos(\sigma_1+\sigma_2))}{9j + 10ml^2 + 2ml^2(3\cos\sigma_1 + 3\cos\sigma_2 + \cos(\sigma_1+\sigma_2))}, \\ f_2 &= \frac{j + 2ml^2 + ml^2(3\cos\sigma_2 + \cos(\sigma_1+\sigma_2))}{9j + 10ml^2 + 2ml^2(3\cos\sigma_1 + 3\cos\sigma_2 + \cos(\sigma_1+\sigma_2))}. \end{aligned}$$

Note that the columns of $A$ are linearly dependent. Moreover, note that the connection for the three link snake has the form described in (9).

### D. Reconstruction equation and base dynamics

Since the first two rows of the connection are zeros, we deduce that the base variables cannot affect the position of the center of mass of the robot. However, the last row of the connection shows a relation between the base variables and the orientation of the robot. Now we would like to generate gaits in the base space in such a way that after a complete cycle, the orientation of the robot is changed, i.e., the phase shift is not zero.

First, we apply nonlinear feedback control to obtain a form of the base equations where direct control on the base variables can be applied. The dynamic equations of motion on the base space, (5), can also be written as

$$\tilde{M}\ddot{r} = -\dot{r}^T\tilde{C}\dot{r} - \tilde{N} + B(r)\tau, \qquad (16)$$

where $\tilde{M}, \tilde{C}$ and $\tilde{N}$ are matrices depending on the base variables $r$ and $\tau = (\tau_1\ \tau_2)^T$ is the vector of control torques [7]. Note that these equations are independent of the group variables for our type of systems. By applying the nonlinear linearizing feedback control $\tau = B(r)^{-1}(\tilde{N} + \dot{r}^T\tilde{C}\dot{r} + \tilde{M}u)$, [3], the base equations have the form[5]

$$\begin{pmatrix} \dot{\sigma_1} \\ \dot{\sigma_2} \end{pmatrix} = \begin{pmatrix} 1 & 0 \\ 0 & 1 \end{pmatrix} \begin{pmatrix} u_1 \\ u_2 \end{pmatrix},$$

where $u = (u_1\ u_2)^T$. By choosing $u_1 = \dot{\sigma}_1$ and $u_2 = \dot{\sigma}_2$ direct control on the base velocities is achieved. As we mentioned earlier, we do not consider the equations for the position variables $x$ and $y$ , as they are constant because of the conservation of linear momentum and the system being isolated and starting from rest. Thus the interesting part of the equations of motion is given as

$$\begin{pmatrix} \dot{\sigma_1} \\ \dot{\sigma_2} \\ \dot{\theta} \end{pmatrix} = \begin{pmatrix} 1 & 0 \\ 0 & 1 \\ f_1(\sigma_1,\sigma_2) & f_2(\sigma_1,\sigma_2) \end{pmatrix} \begin{pmatrix} u_1 \\ u_2 \end{pmatrix}. \qquad (17)$$

### E. Phase Shift

Looking at the last row of the control system, we would like to compute the change in $\theta$ as the base variables $\sigma_1$ and $\sigma_2$ follow a closed trajectory $\partial N$. Integrating the last row and using Stoke's Theorem [8], we get

$$\begin{aligned} \Delta\theta &= \oint_{\partial N} (f_1(\sigma_1,\sigma_2)d\sigma_1 + f_2(\sigma_1,\sigma_2)d\sigma_2), \\ &= \int\int_N \underbrace{\left(\frac{\partial f_1}{\partial \sigma_2} - \frac{\partial f_2}{\partial \sigma_1}\right)}_{F(\sigma_1,\sigma_2)} dA, \end{aligned} \qquad (18)$$

where $N$ is the manifold bounded by $\partial N$. Assuming that the snake links are rods, $j = ml^2/12$, we can compute the integrand in (18) for the three link snake robot.

$$F(\sigma_1,\sigma_2) = \frac{-8(15\sin\sigma_1 + 15\sin\sigma_2 + 11\sin(\sigma_1+\sigma_2))}{(43 + 24\cos\sigma_1 + 24\cos\sigma_2 + 8\cos(\sigma_1+\sigma_2))^2}. \qquad (19)$$

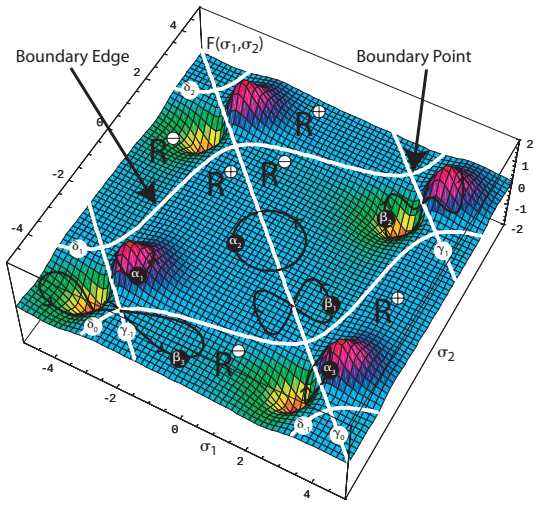


Fig. 2. Three dimensional plot of the integrand in (19) with zero lines and several possible gaits.

Finally, the phase shift can be related to the volume bounded by $F(\sigma_1,\sigma_2)$, the $\sigma_1 - \sigma_2$ plane, and a closed loop which is the desired gait (see Fig. 2).

## V. Gait Synthesis

In this section we will study the integrand in (19) in detail and explain how to generate gaits accordingly.

[4]This is due to the fact that there are no Coriolis terms associated with the translational velocities.

[5]We assume that the base space equations are invertible, i.e. $B$ is an invertible matrix.

### A. Properties of the integrand function

First we notice that $F(\sigma_1, \sigma_2)$ is periodic in both variables, $\sigma_1$ and $\sigma_2$, with period of $2\pi$. Moreover, the function is a hyper odd function, that is

$$F(a+\sigma_1, b+\sigma_2) = -F(a-\sigma_1, b-\sigma_2),\ \forall (a,b) \in K, \quad (20)$$

where $K = \{(k_1\pi, k_2\pi) \text{ such that } k_1, k_2 \in \mathbb{Z}\}$. Using the above two properties we can show that there exist regions in the $\sigma_1 - \sigma_2$ plane where $F(\sigma_1, \sigma_2)$ is either positive or negative. Solving for the zero lines of $F(\sigma_1, \sigma_2)$ we get infinitely many curves due to the periodicity of $F$. Fig. 2 shows such curves labeled by $\gamma_i$'s and $\delta_i$'s. Hence, we have

$$F(p) \begin{cases} = 0, & p \in \gamma_i \text{ or } \delta_i,\ \forall i \in \mathbb{Z}, \\ > 0, & p \in R_{ik}^{\oplus},\ \forall i \text{ even and } i,k \in \mathbb{Z}, \\ < 0, & p \in R_{ik}^{\ominus},\ \forall i \text{ odd and } i,k \in \mathbb{Z}, \end{cases} \quad (21)$$

where $R_{ik}^{\oplus}$ is the region bounded by the curves, $\delta_i$, $\delta_{i+1}$, $\gamma_{i+2k+1}$, and $\gamma_{i+2k+2}$. $R_{ik}^{\ominus}$ is symmetric to $R_{ik}^{\oplus}$ with respect to the origin. Note that the $R_{ik}^{\oplus}$ and the $R_{ik}^{\ominus}$ are congruent, where $F$ is positive on $R_{ik}^{\oplus}$ and negative on $R_{ik}^{\ominus}$.

### B. Gait generation

Given the above properties of the integrand function, we can make three rules for generating gaits:

*1) Closed non-self-intersecting curves:* Any closed non self-intersection curve that lies entirely in one of the regions defined above is guaranteed to produce a phase shift in the fiber direction, $\theta$. The proof is straight forward, integration of a strictly positive (negative) function over a nonzero simply connected region is always positive (negative)[6]. Curve $\alpha_1$ in Fig. 2 belongs to this family of curves.

*2) Closed self-intersecting curves:* Any closed self-intersecting curve will produce a phase shift provided that the curve spans more than one region, the self-intersection occurs along a boundary edge, and the orientation of the curve changes sign as it crosses from one region to another. This will guarantee a nonzero total phase shift since boundary edges are common boundaries of regions with different signs. Curves $\beta_1$ and $\beta_2$ in Fig. 2 belong to this subfamily of curves. However, if the curve's self-intersection occurs at a boundary point, then the curve should maintain the same orientation in both regions. This guarantees a nonzero total phase shift since boundary points separate regions of similar signs. Curve $\beta_3$ in Fig. 2 belongs to this subfamily of curves.

*3) Symmetric curves around the points in the set $K$:* Due to the function being hyper odd over the set of points in $K$, any curve symmetric with respect to points in $K$ will have equal areas in two adjacent regions. Since any two adjacent regions will have opposite values of $F$, integrating over the entire area will yield zero, i.e., no phase shift will be generated along the fiber direction. Referring to Fig. 2, curves $\alpha_2$ and $\alpha_3$ belong to this family of curves.

[6]A sign convention is assumed, since we are integrating over oriented areas.

Note that theoretically, there are no constraints on the shape of the curves described above. For instance, as long as the curve stays entirely in one region, it is guaranteed to generate a nonzero phase shift. The bigger the area enclosed by the curve, the bigger the generated phase shift.

## VI. Simulation Results

In this section we pick several gaits from the above family of gaits and compute the phase shift after a cycle in the base space.

### A. Phase shift computation

We compute the phase shift using two methods: the first is by computing the integral in (18) and the second is by simulating the entire robot motion numerically and compute the phase shift change after one cycle.

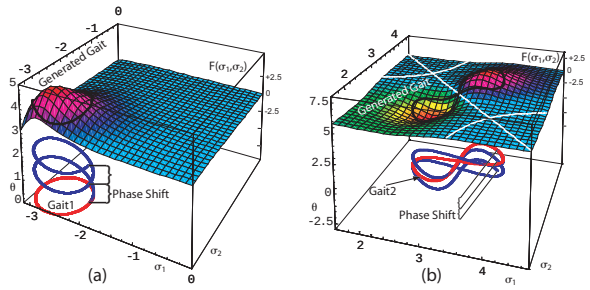


Fig. 3. Simulation of the phase shift for the two gaits, $g_1$(a) and $g_2$(b).

We simulate two gaits, $g_1$ and $g_2$ seen in Fig. 3. Note that $g_1$ belongs to the first family of curves defined above in Section V-B, and $g_2$ belongs to the second family of curves.

$$\begin{aligned} g_1 &: \sigma_1 = 0.5\cos t - 2.64\ ;\ \sigma_2 = 0.5\sin t - 2.64 \\ g_2 &: \sigma_1 = \pi + \frac{0.8}{\sqrt{2}}(\cos t + \frac{\sin 2t}{2})\ ;\ \sigma_2 = \pi + \frac{0.8}{\sqrt{2}}(\cos t - \frac{\sin 2t}{2}) \end{aligned}$$

Now we evaluate the phase shift using the two methods mentioned above to verify our approach,

$$\Delta\theta_1^N = 0.836814\text{rds} \quad ; \quad \Delta\theta_2^N = -0.971484\text{rds} \quad (22)$$

$$\Delta\theta_1^N = 0.836814\text{rds} \quad ; \quad \Delta\theta_2^{\int} = -0.971477\text{rds} \quad (23)$$

Comparing the results in Equations 22 and 23, we deduce that both methods arrive at the same value for the phase shift, $\Delta\theta$.

### B. Optimized gait generation

For synthesizing efficient input gaits, it is possible to perform an optimization. We would like to maximize the phase shift per cycle in the base variables. If we restrict the gaits to lie in one region, then choosing a gait that goes around the boundary of that specific region would produce the maximum phase shift. This is not an optimum solution though, since most of the area enclosed in a region has almost zero height. Hence, a better metric would be to try to maximize the phase shift $\Delta\theta$ while minimizing

the perimeter, $\rho$, of the gait cycle. This would force the gaits to be generated in the vicinity of extrema points in a particular region. So we try to solve the following optimization problem assuming that we choose a region $R \in \mathbb{S} \times \mathbb{S}$, containing the complete input gait:

$$\max_{N \in R} f(\rho, \Delta\theta). \tag{24}$$

where $f(\rho, \Delta\theta)$ is the objective function, depending on $\rho$ and $\Delta\theta$. For the current example we chose $f = \Delta\theta - k \cdot \rho^3$ for a cyclic gait and for different $k$.

Referring to Fig. 4, curves $g_{m3}$, $g_{m4}$, and $g_{m5}$ are optimizations without taking into account the perimeter of the input curve ($k = 0$) and curves $g_{o3}$, $g_{o4}$, $g_{o5}$ are optimization for a nonzero value of $k$. Three different types of gaits were investigated, the circular gait, the elliptical gait, and the self-intersecting gait with the shape of an "eight". For the region of allowable inputs, the square $-6 \leq \sigma_1, \sigma_2 \leq 6$ was chosen.

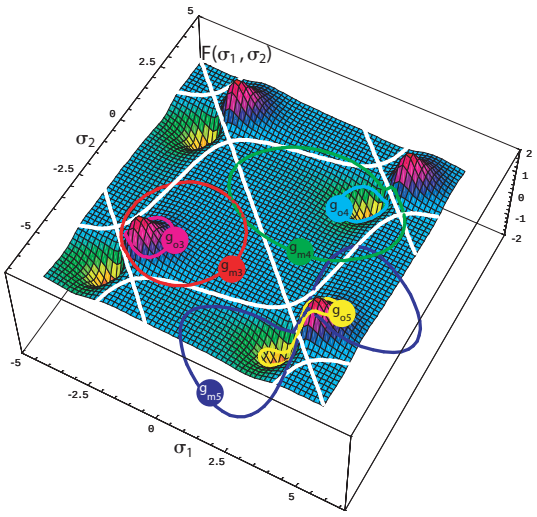


Fig. 4. Several families of optimal gaits.

The computed values of the phase shift versus the perimeter for the three types of optimized gaits can be seen in Table I.

TABLE I

COMPUTED PHASE SHIFT AND PERIMETER OF THE OPTIMIZED GAITS.

| Type | Circle | Circle | Ellipse | Ellipse | Eight | Eight |
|---|---|---|---|---|---|---|
| Fig. 4 | $g_{m3}$ | $g_{o3}$ | $g_{m4}$ | $g_{o4}$ | $g_{m5}$ | $g_{o5}$ |
| $\Delta\theta$ | 2.321 | 1.273 | 2.422 | 1.286 | 4.371 | 1.293 |
| $\rho$ | 12.566 | 4.755 | 15.962 | 4.768 | 25.020 | 5.381 |

Revisiting the computation of other phase shifts done by Walsh in [8] seen in Fig. 1(b), we compute the volume integrals under the gaits devised by Walsh. Not only does our method justify the existence of a local maxima in the value of the phase shift but also allows us to do the same experiment with other types of gaits.

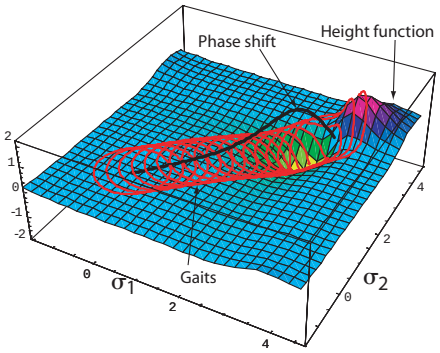


Fig. 5. Gaits proposed by Walsh [8] and the height function that explains the local maxima.

## VII. Conclusion and Future Work

In this paper we were able to naturally design curves in the base space that generated nonzero phase shift along the fiber direction. This is done by equating the phase shift to oriented volume integrals under a well defined height function. Not only does this method allow for a natural way to generate gaits but also to optimize such gaits. We implement this direct gait generation technique to a specific set of robotic systems, particularly, isolated multi-bodied robots that have zero initial momentum and the fiber has an $SE(2)$ group structure. Nonetheless, we have successfully used the same method to generate gaits for principally kinematic systems, i.e., systems whose motion is governed solely by the existence of the "right number" or non-holonomic constraints. We will use both results to generate gaits for more complicated mechanical systems such as the roller racer and the snake board.


## Acknowledgement

We would like to thank Prasad Atkar, Ravi Balasubramanian, Francesco Bullo, David Conner, Jim Ostrowski, and Alfred Rizzi for their time, input and feedback.


## References


[1] Anthony Bloch. *Nonholonomic Mechanics and Control*. Springer Verlag, 2003.

[2] Donald T. Greenwood. *Principles of Dynamics, Second Edition*. Pearson Education, 1987.

[3] Alberto Isidori. *Nonlinear Control Systems (Communications and Control Engineering Series)*. Springer-Verlag, third edition, 1995.

[4] Scott Kelly. *The Mechanics and Control of Robotic Locomotion with Applications to Aquatic Vehicles*. PhD thesis, California Institute of Technology, 1998.

[5] Gabriel Lugo. Differntial geometry in physics. Technical report, University of North Carolina, 1998.

[6] Richard M. Murray and S. Shankar Sastry. Nonholonomic motion planning: Steering using sinusoids. *IEEE T. Automatic Control*, 38(5):700 – 716, May 1993.

[7] J. Ostrowski and J. Burdick. The mechanics and control of undulatory locomotion. *International Journal of Robotics Research*, 17(7):683 – 701, July 1998.

[8] S.S. Walsh, G.C. Sastry. On reorienting linked rigid bodies using internal motions. *Robotics and Automation, IEEE Transactions on*, 11(1):139–146, January 1995.